Theor Chem Acc (2012) 131:1220
DOI 10.1007/s00214-012-1220-0

REGULAR ARTICLE

A simple analysis of the influence of the solvent-induced electronic polarization on the ^{15}N magnetic shielding of pyridine in water

Rodrigo M. Gester · Herbert C. Georg · Tertius L. Fonseca · Patricio F. Provasi · Sylvio Canuto

Received: 13 February 2012 / Accepted: 4 April 2012

Abstract Electronic polarization induced by the interaction of a reference molecule with a liquid environment is expected to affect the magnetic shielding constants. Understanding this effect using realistic theoretical models is important for proper use of nuclear magnetic resonance in molecular characterization. In this work, we consider the pyridine molecule in water as a model system to briefly investigate this aspect. Thus, Monte Carlo simulations and quantum mechanics calculations based on the B3LYP/6-311++G (d,p) are used to analyze different aspects of the solvent effects on the ^{15}N magnetic shielding constant of pyridine in water. This includes in special the geometry relaxation and the electronic polarization of the solute by the solvent. The polarization effect is found to be very important, but, as expected for pyridine, the geometry relaxation contribution is essentially negligible. Using an average electrostatic model of the solvent, the magnetic shielding constant is calculated as −58.7 ppm, in good agreement with the experimental value of −56.3 ppm. The explicit inclusion of hydrogen-bonded water molecules embedded in the electrostatic field of the remaining solvent molecules gives the value of −61.8 ppm.

Keywords NMR · Chemical shielding · Solvent effects · QM/MM · Electronic polarization effects

Dedicated to Professor Marco Antonio Chaer Nascimento and published as part of the special collection of articles celebrating his 65th birthday.

R. M. Gester · S. Canuto (✉)
Instituto de Física, Universidade de São Paulo,
CP 66318, São Paulo, SP 05315-970, Brazil
e-mail: canuto@if.usp.br

R. M. Gester (✉)
Faculdade de Ciências Exatas e Naturais, Universidade Federal do Pará, Marabá, PA 68505-080, Brazil
e-mail: gester@ufpa.br

H. C. Georg · T. L. Fonseca
Instituto de Física, Universidade Federal de Goiás,
CP 131, Goiânia, GO 74001-970, Brazil

P. F. Provasi
Department of Physics, Northeastern University and I-MIT (CONICET), AV. Libertad 5500,
W 3404 AAS Corrientes, Argentina

1 Introduction

Nuclear magnetic resonance (NMR) is one of the most important experimental techniques for characterizing the structure of organic systems [1]. In more recent years, this status has increased in the area of bio-molecular systems [2, 3]. For this reason, it has attracted considerable theoretical and computational interest. As most experiments are made in solution, a proper treatment of the solvent effect is needed. Continuous theoretical developments made in the recent past are making it possible to include solvent effects [4–15] in the calculation of NMR parameters, such as magnetic chemical shielding. The combined use of molecular mechanics and quantum mechanics (QM/MM) is an important alternative.[1] The QM/MM methodology is becoming a realistic method of choice. One successful possibility is the sequential use of Monte Carlo simulation (MC) to generate the liquid structure and QM calculation on statistically representative configurations [16–18]. For the calculation of NMR chemical shielding, it is important

[1] See the special issue dedicated to QM/MM methods in Advances in Quantum Chemistry, 2010, vol. 59.

Published online: 04 May 2012

to understand the role played by the solvent-induced electronic polarization and geometric relaxation of the reference molecule. The first is the change in the electronic distribution of the reference molecule because of the interaction with the solvent [19–25] and the second is the corresponding change in the molecular geometry that accompanies. In this work, we analyze the influence of these two agents in the calculated ^{15}N magnetic chemical shielding constants σ of pyridine in water. There has been several previous studies on the NMR properties of pyridine, and it is used here as a simple test case. Pyridine is part of several important bio-molecules and is amenable to hydrogen bond with water in one specific site. Geometry relaxation of molecules in solution is important for NMR studies because some molecular properties, like indirect spin–spin coupling constants, show extreme sensitivity to the nuclear arrangement [26]. The geometric relaxation in pyridine is small, but it is caused mainly by the hydrogen bond with water in the N site, which adds interest in the $\sigma(^{15}\mathrm{N})$. Of course, this shielding constant has been studied several times before using different methods. Here we focus simply on the effect of the solute polarization by the solvent. To make it simpler, we assume that the reciprocal solvent polarization by the solute is mild and will not be considered. The solute electronic polarization effect can be included using an iterative method [27, 28]. To include these effects and to analyze them separately, we performed two iterative polarization processes, one relaxing only the charge distribution and another relaxing also the geometry, so that we can compare the rigid and relaxed geometry results. The solvent dependence of the nitrogen shielding constant has been systematically analyzed recently [29]. Combination of different continuum models have been used in four different molecules in several different solvents to assess the reliability of continuum models to predict ^{14}N chemical shifts [29]. Although pyridine was not included in this investigation, some common aspects will be seen related to the role of solute polarization and geometry relaxation. In this work, we use the sequential QM/MM methodology to analyze the role of the electronic polarization of the solute due to the solvent and the geometry relaxation in solution in the calculated $\sigma(^{15}\mathrm{N})$ magnetic chemical shielding constants of pyridine in water.

2 Methodology

A sequential QM/MM methodology was applied to study the magnetic shielding constants of hydrated pyridine. In this approach, the liquid configuration is generated first by classical MC simulations. After that, a subset of uncorrelated configurations is sampled and submitted to QM calculations. The MC simulations were carried out in the NPT ensemble with $T = 25$ °C and $P = 1$ atm with one pyridine molecule and 903 waters. The intermolecular interactions were modeled by the Lennard-Jones (LJ) plus Coulomb potential. For the water molecules, we used the TIP3P parameters [30]. For pyridine, the LJ parameters were extracted from the OPLS force field [31], but the atomic charges were obtained for the pyridine in the solvent environment to consider the solute polarization effects. This is done using an iterative procedure [27, 28]. In such iterative polarization scheme, in the QM step, the solute is permitted to relax both its geometry and charge distribution in the presence of the solvent molecules. The atomic charges are obtained using the MP2/aug-cc-pVTZ calculation with the CHELPG (charges from electrostatic potentials using a grid-based method) [32] fitting of the QM electrostatic potential of pyridine. The solvent molecules surrounding the solute are thus permitted to rearrange according to the new solute charge distribution. During the iterative process, the QM calculations are made using the average solvent electrostatic configuration (ASEC) [28]. For constructing the ASEC, we superimpose 250 uncorrelated Monte Carlo configurations in which the pyridine molecule is surrounded by 300 water molecules represented by point charges. This means that all solute-water electrostatic interactions within a distance of 11 Å are taken into account.

The geometry relaxation in the solvent was performed using the Free Energy Gradient (FEG) method [33–35] in conjunction with the sequential QM/MM process. In practice, at each QM step, after calculating the wave function of the solute including the solvent electrostatic interaction, via the ASEC, we calculate the ensemble average of the first and second derivatives of the energy with respect to the solute nuclear positions. These are then used in a Quasi-Newton scheme (here we used the Broyden–Fletcher–Goldfarb–Shanno (BFGS) algorithm [36–40] implemented in the GAUSSIAN 09 package [41]) to obtain a new molecular conformation in the path to the minimum energy structure. The new solute molecular conformation is used to calculate new atomic charges, again using ASEC, and both geometry and charges are updated for a new MC simulation. The iterative process is repeated until the solute dipole moment and geometric parameters converge.

The details of the FEG approach are well described by Nagaoka et al. [33–35], and we have implemented it in a program called Diceplayer [42], which is an interface between the MC program DICE [43] and QM programs. Using this approach, results for the indirect spin–spin coupling and screening constants of liquid ammonia have been obtained in better agreement with experiment [44]. The FEG method has also been successfully employed by Aguilar et al. [45] to find optimized structures of molecules in solution.

The experimental chemical shift of nitrogen in pyridine can be converted to theoretical shielding scale $\sigma(^{14}N)$ using the nitrogen shielding of nitromethane (−135.8 ppm) as in Ref. [46]. Duthaler and Roberts [47] reported a gas-phase shielding of -84.4 ppm, which is corrected to bulk susceptibility. As NMR measurements are difficult in isolated molecules (vacuum or diluted gas-phase condition), it is common to use the cyclohexane solvent to approximate the vacuum ambient. Duthaler and Roberts also reported a value of −82.9 ppm after considering bulk susceptibility corrections and the extrapolation to infinite dilution. However, comparisons with the theoretical results for the isolated molecule show some discrepancies. Our present results using the B3LYP model with the specially designed aug-pcS-n ($n = 1, 2, 3$) basis sets [48] for the isolated pyridine give results for the nitrogen chemical shielding varying between −110.2 and −117.2 ppm. This is far from the gas-phase experiment above [47] with large differences varying between 25.8 and 32.8 ppm. This discrepancy suggests comparison with other quantum chemistry methods and we have also calculated the in-vacuum isolated $\sigma(^{14}N)$ values using the random phase approximation (RPA) [49] and the second-order polarization propagation approximation (SOPPA) [50] as implemented in DALTON program [51]. For instance, using the aug-pcS-2[2] and aug-cc-pVTZ-J [52–56] basis sets, our RPA results give shielding constants of −115.8 and −104.7 ppm, respectively. Our SOPPA/aug-cc-pVTZ-J calculation gives −103.6 ppm for the chemical shielding, what differs appreciably from experiment. Mennucci and collaborators [5] have recently used the B3LYP/6-311+G(d,p) level of theory to obtain a nitrogen nuclear shielding of −102.8 ppm for isolated pyridine. Using the same level of theory, we obtained −103.5 ppm. Thus, there are clear indications that the results for the isolated molecule obtained by theory and experiment show some inconsistencies. Therefore, in this study, we only report the calculated results in aqueous environment.

DFT methods and basis sets have been widely used to calculate magnetic shieldings and spin–spin couplings [15, 20, 57–62]. In this work, we employ the same B3LYP/6-311+G(d,p) model successfully used by Mennucci et al. [5] using the gauge independent atomic orbital (GIAO) [63, 64] approximation to calculate the magnetic constants. In this work, we use the CHELPG scheme for obtaining the atomic charges, and the calculations are performed within the GIAO model both implemented in the GAUSSIAN 09 package [41].

[2] The aug-cc-pVTZ-J basis sets can be downloaded from https://bse.pnl.gov/bse/portal.

3 Results

3.1 Solute polarization

Table 1 shows the calculated and experimental dipole moments of pyridine isolated and in water. The calculated MP2/aug-cc-pVTZ value of 2.33 D is in good agreement with the experimental result of 2.15 ± 0.05 D [65]. The geometry of isolated pyridine obtained at the same MP2/aug-cc-pVTZ level is also in very good agreement with experiment. The N_1–C_2 bond length is calculated as 1.341 Å, whereas the C_2–C_3 and C_3–C_4 bonds are 1.393 and 1.391 Å, respectively, compared with the experimental values of 1.340, 1.395 and 1.394 Å [66] (atomic indices are shown in Fig. 1).

Experimental reports on liquid-phase molecular dipole moments are scarce, because of the natural difficulty of a direct measurement. Theoretical reports can be found only for the pyridine-water clusters [67, 68]. Here, we investigate the solute polarization by the solvent that implies an increase in its dipole moment. This is obtained using continuum and discrete solvent models. The continuum approach uses the polarized continuum model [69] (PCM), while the discrete solvent model uses the solvent molecules treated as point charges only. The iterative polarization is

Table 1 The dipole moment of pyridine calculated at the MP2/aug-cc-pVTZ level of theory

	Isolated		In solution		
	Calc.	Exp. [65]	PCM	Discrete rigid	Discrete relaxed
μ	2.33	2.15 ± 0.05	3.41	3.94	4.38

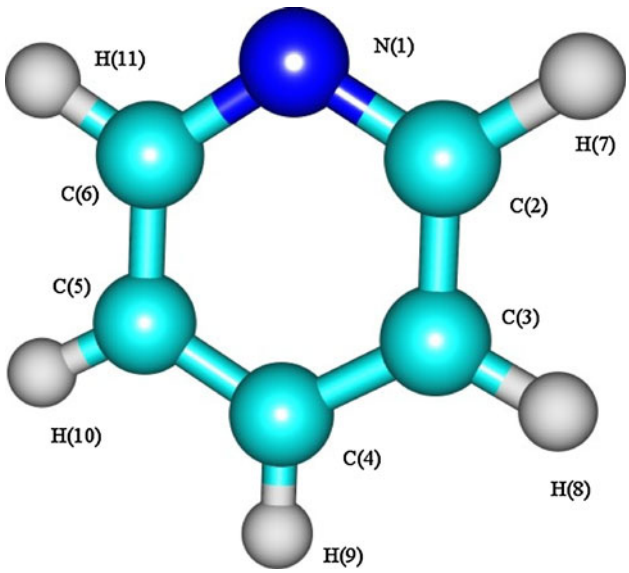

Fig. 1 Pyridine geometry and atomic labels used

used here with and without geometry relaxation, as described in the previous section. The convergence of the calculated value for the rigid case is shown in Fig. 2 for illustration. Table 1 summarizes the results. The PCM approach obtains a dipole moment of pyridine in water of 3.41 D, which represents an increase of 46 % as compared with the gas-phase result. With the iterative scheme representing the solvent as point charges, we obtain dipole moments of 3.94 (increase of 69 %) and 4.38 D (increase of 88 %) for the rigid and relaxed geometries, respectively. The change in geometry is mild, as seen before in similar nitrogen-containing molecules [29], but still affects the calculated dipole moment. We analyze next the influence of this polarization in the solute–solvent hydrogen bonds in the charge on the nitrogen site and hence how these affect the σ (^{15}N) in water.

3.2 Hydrogen bonds

Considering the rigid model of pyridine, we now briefly discuss the effect of the polarization in the coordination of water molecules around the solute. In the unpolarized situation, we obtain the corresponding coordination of 1.62 water molecules. In the polarized case, this coordination changes to 2.02. These coordinated water molecules are not assured to be hydrogen bonded to pyridine. Thus, in addition to the geometric, we have used also an energetic criterion [67, 70, 71] derived from the pairwise interaction energy. This is shown Fig. 3. Thus, for the polarized case, we consider a hydrogen bond when the $R_{N-O} \leq 3.5$ Å, the angle α(N–OH) $\leq 35°$ and the interaction energy is <-4.0 kcal mol. This geometric criterion is obtained from the radial and angular distribution functions, and the energy

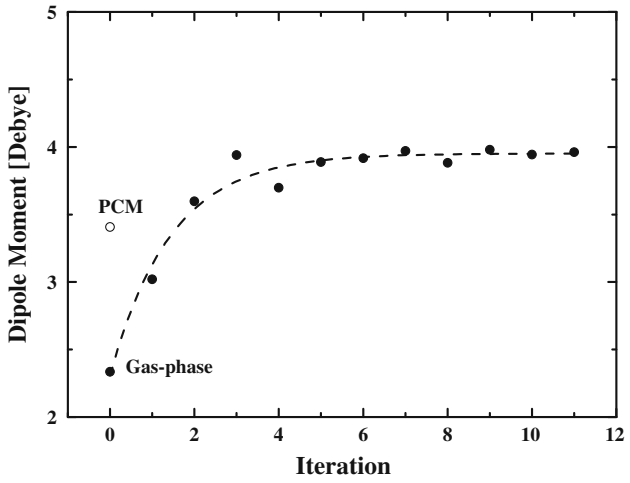

Fig. 2 The calculated dipole moment of isolated and hydrated pyridine. The *empty circle* shows the polarized continuum model prediction. The *black circles* represent the iterative values with rigid geometry, starting from the gas phase

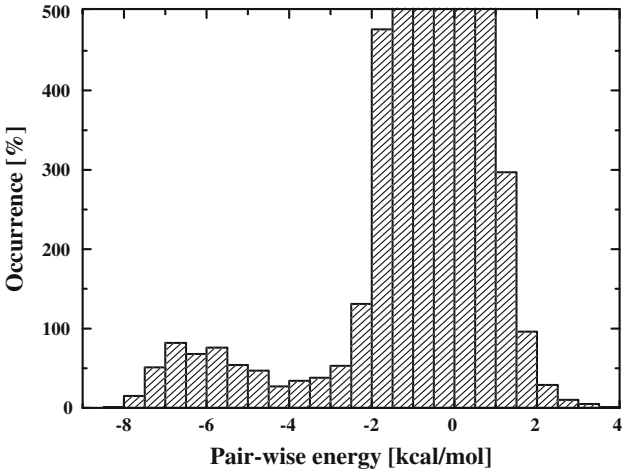

Fig. 3 Histogram of the pairwise interaction energy between rigid pyridine and water in the polarized case

criterion is obtained from the pairwise interaction energy distribution (see Fig. 3). Similar analysis is made for the unpolarized case, where the $R_{N-O} \leq 3.2$ Å, α(N–OH) $\leq 35°$ and the interaction energy is <-3.0 kcal/mol. In the polarized case, we find that 2 % of the configurations make no hydrogen bonds, whereas 36.4 % make one hydrogen bond. The most probable situation corresponds to 60.4 % of the configurations making 2 hydrogen bonds. In the average, as can be seen in Table 2, we find 1.6 hydrogen bonds between the nitrogen atom of pyridine and the hydrogen atom of water. This is considerably larger than the unpolarized situation (0.71 hydrogen bonds) and somewhat larger than using the original point charges of the OPLS model (1.1).

3.3 Chemical shielding

In the following theoretical analysis, we separate the different contributions, and we first analyze the electrostatic part. The PCM and the electrostatic (ASEC) models give the results shown in Table 3. For comparison with experiments, we considered the early measurements of the ^{15}N

Table 2 Statistics of the hydrogen bonds formed between pyridine and water

HBs	Occurrence (%)		
	[Ref. [68]]	Unpolarized[a]	Polarized[a]
0	17	36	2
1	62	56.8	36.4
2	20	7.2	60.4
3	1	0	1.2
Average	1.1	0.71	1.61

[a] Both polarized and unpolarized models use a rigid geometry of pyridine. 250 uncorrelated configurations were analyzed

Table 3 The effects of the solute polarization and geometry relaxation on the calculated nuclear magnetic shielding constant

	σ (^{15}N) in water	
	Rigid	Relaxed
Unpolarized	−82.1	−78.0
Polarized	−59.8	−58.7
PCM[a]	−81.0	
Liquid (Exp.)[b]		−56.3

The magnetic constants are calculated at the B3LYP/6-311+G(d,p) level, while the pyridine (rigid and relaxed) geometries are obtained with the MP2/aug-cc-pVTZ level

[a] The PCM value was obtained using the gas-phase MP2/aug-cc-pVTZ geometry

[b] In cyclohexane solution [59], this value is corrected to susceptibility effects and extrapolated to infinite dilution

shielding constants in solvated pyridine due to Duthaler and Roberts [59]. They report a magnetic shielding in water of −59.9 ppm. After including bulk susceptibility corrections, this value changes to −56.3 ppm. The continuum PCM model estimates a shielding of −81.0 ppm, which differs by 24.3 ppm from the experiment.

We now analyze the polarization effects on the σ (^{15}N). The polarization effect using a fixed geometry is shown in Fig. 4. It can be noted that the theoretical result improve systematically until convergence in the theoretical value of −59.8 ppm, in very good agreement with the experimental value of −59.9 ppm (or −56.3 ppm if correcting for the bulk susceptibility). It is then found here that the polarization effect has a great influence on the calculated value of the magnetic shielding of the nitrogen atom of pyridine in water. Combining the polarization and geometric effects gives the theoretical value of −58.7 ppm. Thus, the separate geometric effect is only −1.1 ppm. This has two components. One is the direct change in the geometry that affects the local magnetic shielding. The other is the indirect contribution that comes from the change in the dipole moment and therefore the coordination of solvent molecules. The combined effect is seen to be very small. The geometric variation is expected to be small, and indeed the largest deviation found is a small increase of the $R(N_1–C_6)$ by 0.006 Å and a decrease in the $A(C_2N_1C_6)$ angle by 0.1°. Contreras and Peralta [72] have shown that for ammonia, the larger contribution to the spin–spin coupling arises mainly from the angle variations. But overall, the present calculations show that geometric effect on the chemical shielding σ (^{15}N) of pyridine in water is very mild, as also noted before [29] for similar systems.

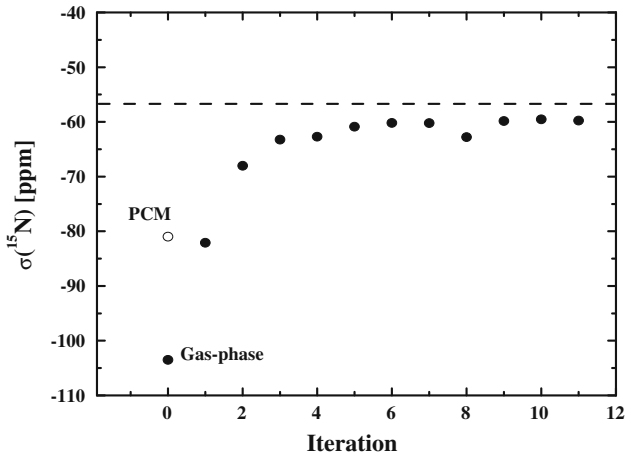

Fig. 4 The evolution of the calculated σ(^{15}N) as a function of the iteration steps obtained for rigid pyridine simulation. The experimental data is shown as the *dotted line*

Having analyzed the electrostatic contribution to the magnetic shielding, we now consider the exchange and the van der Waals contributions by considering some explicit solvent water molecules around the reference pyridine molecule. For a systematic consideration, we analyze first the role of the hydrogen-bonded (HB) water molecules. The results are shown in the Table 4. As the results shown above have indicated that the geometry relaxation is unimportant, all calculations are now performed using the Monte Carlo configurations obtained considering the rigid pyridine geometry. The magnetic shielding on the nitrogen atom using only the HB water molecules explicitly is −83.4 ± 0.7 ppm, a value that differs from experiment by ∼27 ppm. These calculations are made on the structures previously extracted and use different number of water molecules for each configuration (Table 2). An improvement in the model can be obtained by embedding theses

Table 4 The calculated B3LYP/6-311+G(d,p) and experimental ^{15}N magnetic shielding constants [ppm] in hydrated pyridine

σ (^{15}N) in water					
PCM[a]	ASEC[b]	HB[c]	HB+PC[d]	$6H_2O$+PC[e]	Exp.[f]
−81.0	−59.8 (−58.7)	−83.4 ± 0.7	−62.4 ± 0.7	−61.8 ± 0.9	−56.3 (−59.9)

[a] The PCM values were obtained using the isolated MP2/aug-cc-pVTZ geometry

[b] The values in parenthesis were obtained from in-water relaxed geometry

[c] HB includes only the explicit pyridine-water hydrogen bonds. See text

[d] HB+PC includes the explicit pyridine-water hydrogen bonds and the remaining 320 water molecules treated as point charges. See text

[e] $6H_2O$+SPC includes the pyridine surrounded by the six water nearest the pyridine nitrogen. The remaining 303 water molecules were included as point charges. See text

[f] Value corrected [uncorrected] for bulk susceptibility effects and extrapolated to infinite dilution [59]

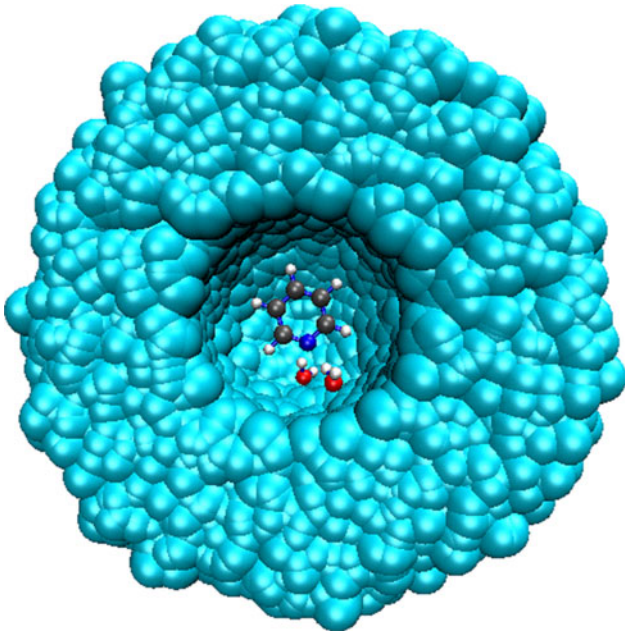

Fig. 5 Pyridine-water hydrogen-bonded complex embedded in the electrostatic field of the remaining water molecules

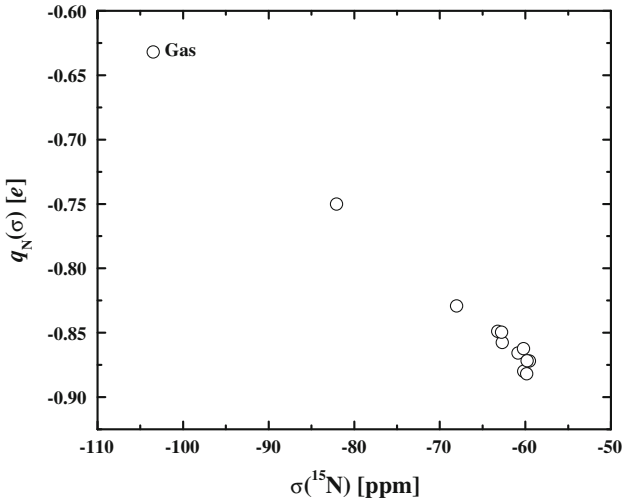

Fig. 6 The electronic charge on the nitrogen atom as a function of the magnetic shielding

hydrogen-bonded structures in the electrostatic field of the remaining water molecules. This model is termed HB+PC, and the situation is illustrated in Fig. 5 that shows one of the configurations used for the calculations of the magnetic shielding. The water molecules in the embedding enter only with their point charges located in the atomic position as described by the TIP3P potential. In HB+PC, a total of 320 water molecules are included as point charges. The calculated chemical shielding is now -62.4 ± 0.7 ppm in fair agreement with the experimental result of -56.3 ppm. This result differs from the simple ASEC electrostatic result by less than 3 ppm. Increasing further the number of explicit water molecules, we see that using six explicit solvent molecules in the electrostatic embedding ($6H_2O$+PC) gives a close result of -61.8 ± 0.7 ppm, only 0.6 ppm of difference with the HB+PC result, showing that the principal contribution comes from the pyridine-water hydrogen bonds plus electrostatic contribution. This is in line with a previous study on diazines [7] where it is concluded that a few explicit solvent molecules would be appropriate, but the most important contribution derives from the long-range electrostatic interaction, as noted before [5].

Finally, we analyze the influence of the polarization in the atomic charge on the nitrogen site. Figure 6 shows that the polarization has a marked influence on the nitrogen charge and this clearly associates with the variations of the magnetic shielding results. One can observe that the correlation is essentially linear with an increase of $q_N(\sigma)$ correlating with the decrease of the magnetic shielding.

4 Conclusions

This work analyses the solute electronic polarization induced by the interaction with water solvent and its implications on the σ (^{15}N) magnetic shielding constant of pyridine. For the isolated pyridine molecule, the dipole moment obtained at the MP2/aug-cc-pVTZ level is 2.33 D, which is close to the experimental value (2.15 ± 0.05 D). In aqueous environment, values varying from 3.41 to 4.38 D were obtained showing some considerable polarization. The influence of this solute electronic polarization on the σ (^{15}N) is calculated. It is seen that the electronic polarization has a great influence in the number of solute–solvent hydrogen bonds and in the atomic charges. Using an iterative procedure to equilibrate the solute charges with the solvent electrostatic field, it is seen that the calculated values of the σ (^{15}N) magnetic shielding constant of pyridine converges to a value that is in close agreement with the experimental value. These variations in the σ (^{15}N) correlate well with the changes in the atomic charge on the nitrogen site. These aspects indicate a redistribution of the solute charges due to the solvent that although not directly observable may be a sensitive probe of the solute polarization due to the solvent and has been of recent and fundamental interest [29, 73–75]. The best result of -61.8 ppm obtained here corresponds to the electronically polarized pyridine surrounded by six water molecules and this entire system embedded in the electrostatic field of the remaining water molecules, and is in good agreement with the experimental results of -56.3 and -59.9 ppm. The solvent shift is, however, overestimated, and we attribute this to uncertainties in the vacuum results.

Acknowledgments This work is partially supported by CNPq, CAPES and FAPESP (Brazil). Additional support from the INCT-FCx (Institute for Complex Fluids) and NBioNet are gratefully acknowledged. RMG thanks CNPq for a doctoral fellowship and P. F. P. thanks UNNE (PICTO-UNNE-227 BID 1728/OC-AR) and CONICET (Argentina).

References

1. Hore PJ (1995) Nuclear magnetic resonance. Oxford University Press, New York
2. Canuto S (ed) (2008) Solvation effects on molecules and biomolecules. Computational methods and applications. Springer, New York
3. Mennucci B, Cammi R (eds) (2007) Continuum solvation models in chemical physics. Wiley, New York
4. Buckingham AD, Schafer T, Schneider WG (1960) J Chem Phys 32:1227
5. Mennucci B, Martinez JM, Tomasi J (2001) J Phys Chem A 105:7287
6. Mennucci B (2002) J Am Chem Soc 124:1506
7. Kongsted J, Mennucci B (2007) J Phys Chem A 111:9890
8. Malkin VG, Malkina OL, Steinebrunner G, Huber H (1996) Chem Eur J 2:452
9. Chesnut DB, Rusiloski BE (1994) J Mol Struct 314:19
10. Cheeseman JR, Trucks GW, Keith TA, Frisch MJ (1996) J Chem Phys 104:5497
11. Fileti EE, Georg HC, Coutinho K, Canuto S (2007) J Braz Chem Soc 18:74
12. Kongsted J, Aidas K, Mikkelsen KV, Sauer SPA (2008) J Chem Theory Comput 4:267
13. Møgelhøj A, Aidas K, Mikkelsen KV, Sauer SPA, Kongsted J (2009) J Chem Phys 130:134508
14. Ligabue A, Sauer SPA, Lazzeretti P (2007) J Chem Phys 126:154111
15. Keal TW, Helgaker T, Salek P, Tozer DJ (2006) Chem Phys Lett 425:163
16. Coutinho K, Canuto S (2000) J Chem Phys 113:9132
17. Coutinho K, Canuto S, Zerner MC (2000) J Chem Phys 112:9874
18. Canuto S, Coutinho K, Trzresniak D (2003) Adv Quantum Chem 41:161
19. Fonseca TL, Coutinho K, Canuto S (2008) J Chem Phys 129:034502
20. Manzoni V, Lyra ML, Gester RM, Coutinho K, Canuto S (2010) Phys Chem Chem Phys 12:14023
21. Aidas K, Møgelhøj A, Kjaer H, Nielsen CB, Milkkelsen KV, Ruud K, Christiansen O, Kongsted J (2007) J Phys Chem A 111:4199
22. Pranata J, Wierschke SG, Jorgensen WL (1991) J Am Chem Soc 113:2810
23. Gao J, Xia X (1992) Science 258:631
24. Jorgensen WL (ed) (2007) J Chem Theor Comput special issue 3:1877–2145
25. Dahlke EE, Truhlar DG (2007) J Chem Theor Comput 3:46
26. Elguero J (2007) Magn Reson Chem 46:356
27. Georg HC, Coutinho K, Canuto S (2006) Chem Phys Lett 429:119
28. Coutinho K, Georg HC, Fonseca TL, Ludwig V, Canuto S (2007) Chem Phys Lett 437:148
29. Ribeiro RF, Marenich AV, Cramer CJ, Truhlar DG (2009) J Chem Theor Comput 5:2284
30. Jorgensen WL, Chandrasekhar J, Madura JD, Impey RW, Klein ML (1983) J Chem Phys 79:926
31. Jorgensen WL, McDonald NA (1998) J Mol Struc 424:145
32. Breneman CM, Wiberg KB (1990) J Comput Chem 11:361
33. Okuyama-Yoshida N, Nagaoka M, Yamabe T (1998) Int J Quantum Chem 70:95
34. Okuyama-Yoshida N, Kataoka K, Nagaoka M, Yamabe T (2000) J Chem Phys 113:3519
35. Hirao H, Nagae Y, Nagaoka M (2001) Chem Phys Lett 348:350
36. Broyden CG (1970) IMA J Appl Math 6:76
37. Fletcher R (1970) Comput J 13:317
38. Goldfarb D (1970) Math Comput 24:23
39. Shanno DF (1970) Math Comput 24:647
40. Shanno DF, Kettler PC (1970) Math Comput 24:657
41. Frisch MJ, Trucks GW, Schlegel HB, Scuseria GE, Robb MA, Cheeseman JR, Scalmani G, Barone V, Mennucci B, Petersson GA, Nakatsuji H, Caricato M, Li X, Hratchian HP, Izmaylov AF, Bloino J, Zheng G, Sonnenberg JL, Hada M, Ehara M, Toyota K, Fukuda R, Hasegawa J, Ishida M, Nakajima T, Honda Y, Kitao O, Nakai H, Vreven T, Montgomery JJA, Peralta JE, Ogliaro F, Bearpark M, Heyd JJ, Brothers E, Kudin KN, Staroverov VN, Kobayashi R, Normand J, Raghavachari K, Rendell A, Burant JC, Iyengar SS, Tomasi J, Cossi M, Rega N, Millam JM, Klene M, Knox JE, Cross JB, Bakken V, Adamo C, Jaramillo J, Gomperts R, Stratmann RE, Yazyev O, Austin AJ, Cammi R, Pomelli C, Ochterski JW, Martin RL, Morokuma K, Zakrzewski VG, Voth GA, Salvador P, Dannenberg JJ, Dapprich S, Daniels AD, Farkas O, Foresman JB, Ortiz JV, Cioslowski J, Fox DJ (2004) Gaussian 03, Revision D 02. Wallingford, Gaussian
42. Georg HC, Canuto S (2009) Diceplayer. University of São Paulo, São Paulo
43. Coutinho K, Canuto S (2009) DICE (version 2.9): a general monte carlo program for liquid simulation. University of São Paulo, São Paulo
44. Gester RM, Georg HC, Canuto S, Caputo MC, Provasi PF (2009) J Phys Chem A 113:14936
45. Galván IF, Sánchez ML, Martin ME, Olivares del Valle FJ, Aguilar MA (2003) J Chem Phys 118:255
46. Facelli JC (2000) Chem Phys Lett 322:91
47. Duthaler RO, Roberts JD (1978) J Am Chem Soc 100:4969
48. Jensen F (2008) J Chem Theory Comput 4:2008
49. Christiansen O, Bak KL, Koch H, Sauer SPA (1998) Chem Phys Lett 284:47
50. Provasi PF, Aucar GA, Sauer SPA (2001) J Chem Phys 115:1324
51. DALTON, a molecular electronic structure program, Release Dalton2011 (2011)
52. Bak KL, Koch H, Oddershede J, Christiansen O, Sauer SPA (2000) J Chem Phys 112:4173
53. Nielsen ES, Jørgensen P, Oddershede J (1980) J Chem Phys 73:6238
54. Packer MJ, Dalskov EK, Enevoldsen T, Jensen HJA, Oddershede J (1996) J Chem Phys 105(14):5886
55. Sauer SPA (1996) Chem Phys Lett 260:271
56. Enevoldsen T, Oddershede J, Sauer SPA (1998) Theor Chem Acc 100:275
57. Keal TW, Tozer DJ (2004) J Chem Phys 121:5654
58. Auer AA (2009) Chem Phys Lett 467:230
59. Becke AD (1993) J Chem Phys 98:5648
60. Lee C, Yang W, Parr RG (1988) Phys Rev B 37:785
61. Adamo C, Barone V (1999) J Chem Phys A 110:6158
62. Alkorta I, Elguero J (2004) Magn Reson Chem 42:955
63. Gauss J (1993) J Chem Phys 99:3629
64. Wolinski K, Hinton JF, Pulay P (1990) J Am Chem Soc 112:8251
65. DeMore BB, Wilcox WS, Goldstein JH (1954) J Chem Phys 22:876
66. Lide DR (1992) Handbook of chemistry and physics, 73rd edn. CRC Press, Boca Raton
67. Fileti EE, Coutinho K, Malaspina T, Canuto S (2003) Phys Rev E 67:061504

68. Malaspina T, Coutinho K, Canuto S (2002) J Chem Phys 117:1692
69. Miertuš S, Scrocco E, Tomasi J (1981) Chem Phys 55:117
70. Stilinger FH, Rahman A (1974) J Chem Phys 60:3336
71. Mezei M, Beveridge DL (1981) J Chem Phys 74:622
72. Contreras RH, Peralta JE (2000) Prog Nucl Magn Reson Spectrosc 37:321
73. Zhan C-G, Chipman DM (1999) J Chem Phys 110:1611
74. Curutchet C, Cramer CJ, Truhlar DG, Ruiz-Lopez MF, Rinaldi D, Orozco M, Luque FJ (2003) J Comput Chem 24:284
75. Marenich AV, Olson RM, Chamberlin AC, Cramer CJ, Truhlat DG (2007) J Chem Theory Comput 3:2055